

# Perpendicular giant magnetoresistance of electrodeposited Co/Cu-multilayered nanowires in porous alumina templates

X.-T. Tang<sup>a)</sup> and G.-C. Wang

*Department of Physics, Applied Physics and Astronomy, Rensselaer Polytechnic Institute, Troy, New York 12180-3590*

M. Shima

*Department of Materials Science and Engineering, Rensselaer Polytechnic Institute, Troy, New York 12180-3590*

(Received 4 September 2005; accepted 16 December 2005; published online 7 February 2006)

The giant magnetoresistance (GMR) of multilayered Co/Cu nanowires potentiostatically electrodeposited inside the pores of an anodized alumina template was studied in the current perpendicular to the plane (CPP) geometry. The maximum magnetoresistance change of 13.5% was observed for Co(8 nm)/Cu(10 nm) nanowires at room temperature. The interfacial roughness and/or an intermixing between Co and Cu layers were varied by changing the Cu deposition potential. However, the CPP-GMR value only slightly decreases as the Cu deposition potential increases to the positive value. This indicates that the interfacial roughness and/or intermixing are not a crucial factor in determining the CPP-GMR value of the Co/Cu nanowires, which is argued to be due to the uncoupled magnetic layers. The x-ray diffraction shows that Co/Cu nanowires with 300 nm diameter have a face-centered-cubic structure with a strong (111) texture along the wire axes; their magnetic easy axes are perpendicular to the wire axes as determined from the CPP-GMR curve. The effects of the interface roughness and/or an intermixing between Co and Cu layers and their thickness variation on the CPP-GMR are discussed. © 2006 American Institute of Physics.

[DOI: [10.1063/1.2168290](https://doi.org/10.1063/1.2168290)]

## I. INTRODUCTION

Magnetotransport properties of low-dimensional magnetic systems have been extensively studied in the last decades because of their importance for device applications such as ultrahigh-density data storage as well as for scientific exploration of spin transport phenomena in low-dimensional systems which are often very different from those of bulk or thin films.<sup>1</sup> Particularly, multilayered nanowires consisting of alternating magnetic and nonmagnetic layers are an ideal system to investigate the giant magnetoresistance (GMR) effect in the current perpendicular to plane (CPP) geometry because the high aspect ratio of the multilayered wire leads to a larger resistance that enables high accuracy in the measurement. In the CPP geometry, due to the spin accumulation effect, the scaling length which governs the GMR effect is the spin-diffusion length, which can be much larger than electron mean free path;<sup>2</sup> CPP-GMR effect should be observed in multilayered nanowires with a large layer thickness of either a nonmagnetic or magnetic layer. This is in contrast to multilayered thin films where the current in the plane (CIP)-GMR has been generally observed for small layer thickness.

Magnetic nanowires with the diameter of a few tens to a few hundreds nanometers can be made by growing them in highly ordered pores of a suitable template such as anodized alumina and polycarbonate templates.<sup>3-5</sup> Using electrodeposition, metal/metal multilayers in the film format such as

Co/Cu can be grown by alternating the reduction potential for each metal layer in an electrolytic solution containing both the ionic species.<sup>6-8</sup> Therefore by combining the single-bath electrodeposition method for multilayer film growth with the use of a nanoporous template, an array of multilayered nanowires can be prepared.<sup>9-11</sup>

It has been shown that a significant intermixing can occur by an exchange reaction between nonmagnetic (Cu) and magnetic (Co) layers of Co/Cu multilayer films during the growth in a single bath by pulsed electrodeposition.<sup>12-16</sup> Also, It has been reported that the GMR effect in magnetic multilayer films often depends on the layered structure including the interfacial roughness.<sup>7,8</sup> However, the effects of interfacial roughness of magnetic multilayers thin films on the GMR effect have controversial results: as the interfacial roughness increases, larger GMR effects have been observed in some multilayer films systems such as Fe/Cr,<sup>17,18</sup> while smaller GMR effects have been found in other films systems such as Co/Cu.<sup>19,20</sup> In this work, we study the effects of interfacial roughness and intermixing on the CPP-GMR effect in the Co/Cu nanowires by varying the Cu deposition potential. We have found that in Co/Cu multilayered wires of  $\sim 300$  nm in diameter and  $\sim 60$   $\mu\text{m}$  in length, the Cu deposition potential has a strong effect on the exchange reaction, thus results in different interface roughness. The CPP-GMR value only slightly decreases as the interface roughness increases. But the shape of the CPP-GMR curve changes, in the sense that both the saturation field and the peak position value increase as the interface roughness increases. A maximum magnetoresistance (MR) change of

<sup>a)</sup>Electronic mail: [tangx@rpi.edu](mailto:tangx@rpi.edu)

13.5% was observed at room temperature for Co(8 nm)/Cu(10 nm) nanowires. We also discuss the optimum Co and Cu layer thicknesses that yield the largest CPP-GMR, the correlations between the CPP-GMR and Co layer thicknesses, and the magnetic easy axis.

## II. EXPERIMENT

### A. Electrodeposition of multilayered Co/Cu nanowires

Electrodeposition of Co/Cu nanowires was carried out potentiostatically in a single bath using a classical three-electrode system including a Ag/AgCl reference electrode and a platinum counter electrode. The deposition potential  $U$  was controlled with respect to the reference electrode. An electrolytic solution containing 1.5M CoSO<sub>4</sub>·7H<sub>2</sub>O, 0.5M H<sub>3</sub>BO<sub>3</sub>, and 0.008M CuSO<sub>4</sub>·5H<sub>2</sub>O in the bath was maintained at the pH of 3.5 at room temperature during the growth of Co/Cu nanowires. Commercial anodized alumina templates (Whatman, Anodisc) of 60 μm in thickness and 100 nm in nominal pore size were utilized for this study. According to the information supplied by the vendor, each 60-μm-long pore consists of continuously connected two portions: one end has pores of 100 nm in diameter and 1–2 μm in length and the other end with pores of 300 nm in diameter and 58–59 μm in length. The detailed structure of the templates is described elsewhere.<sup>3</sup> Prior to electrodeposition of Co/Cu nanowires, a 1-μm-thick Cu film was coated onto the 300 nm pore side of the template using electron-beam evaporation. The coated Cu film served as a conducting electrode for electrodeposition of Co and Cu layers. A thin gold film (40–60 nm) was then grown on the 100 nm pore side of the template using a thermal evaporator. The Au film was utilized to detect a sudden increase of the deposition current when the growing nanowires reached the end of the pores.

To determine the optimum deposition potentials for Co and Cu layers, cyclic voltammetry was performed using the electrolyte solution containing Co and Cu species. In the measurements, the deposition processes of both Co and Cu and the subsequent dissolution process of Co were specifically monitored. When the potential  $U$  was swept to the larger negative values, an onset of nucleation and growth of copper were observed as a cathodic current at  $U=0.1$  V, while Co began to be deposited at  $U=-0.7$  V, as shown in Fig. 1(a). When the potential was reversed above  $U=-0.35$  V, an onset of Co stripping was detected as an anodic current. Growth of Co/Cu nanowires was carried out by alternating the deposition potential between  $U=-0.3$  or  $-0.5$  V for Cu and  $-1.0$  V for Co. We chose the Cu deposition potential at either  $-0.3$  or  $-0.5$  V to study the effects of the interface roughness and/or intermixing on the CPP-GMR. The nanowire growth was stopped as soon as a sudden increase of current was detected, indicating that the growing nanowires have reached the end of the pores. A typical chronoamperometric curve is shown in Fig. 1(b) along with the applied potential change. The positive current peak observed at the beginning of each Cu deposition period is due to dissolution of Co and a concurrent exchange reac-

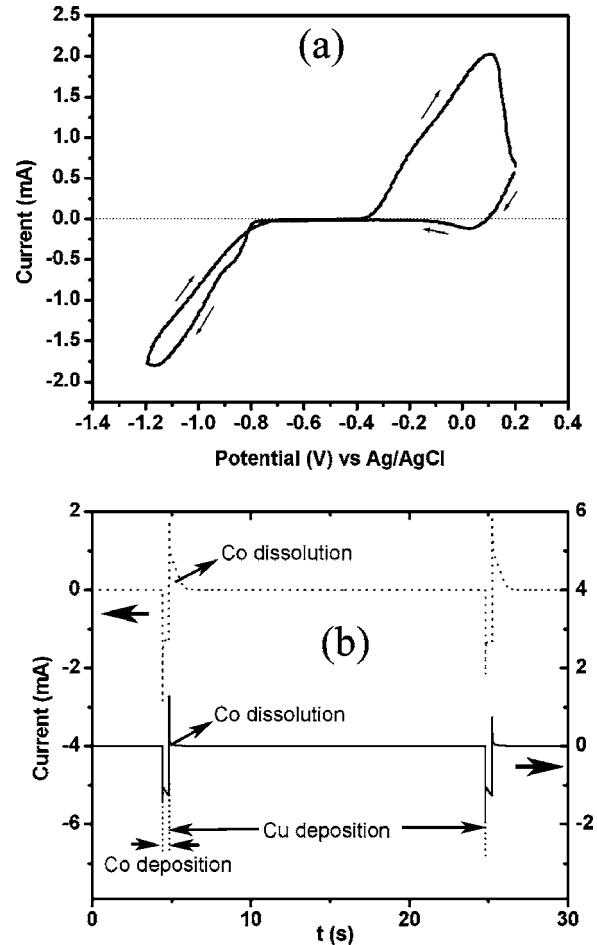


FIG. 1. (a) Cyclic voltammogram measured for the Co–Cu electrolytic solution used for electrodeposition of multilayered Co/Cu nanowires and (b) current transients measured for electrodeposition at  $-1.0$  V for Co and  $-0.3$  V for Cu (dashed curve) and for growth at  $-1.0$  V for Co and  $-0.5$  V for Cu (solid curve). The Co dissolution peaks at the beginning of Cu deposition are indicated by the tilted arrows. The degree of Co dissolution is higher at  $-0.3$  V Cu potential than that at  $-0.5$  V Cu potential. The thicker horizontal arrows refer to deposition currents with different vertical scales.

tion between Cu and Co at the growing surface. It is seen that the anodic dissolution of Co is negligibly small at  $U=-0.5$  V for the Cu deposition, but significant at  $U=-0.3$  V.

To determine the nominal thicknesses for Cu and Co layers, the bilayer thickness was first calculated by dividing the length of multilayered nanowire  $l$  and the number of periods  $N$ , that is,  $l_{\text{bilayer}}=l_{\text{Cu}}+l_{\text{Co}}=l_{\text{nanowire}}/N_{\text{periods}}$ . Then, the thickness ratio of the Cu to Co layers was estimated from the cumulative electric charges used for electrodeposition of individual Cu layers ( $Q_{\text{Cu}}$ ) and Co layers ( $Q_{\text{Co}}$ ), namely,  $l_{\text{Cu}}/l_{\text{Co}}=(36.7\eta_{\text{Cu}}Q_{\text{Cu}})/(34.3\eta_{\text{Co}}Q_{\text{Co}})$ . The constant values of 36.7 and 34.3 are determined based on Faraday's law.<sup>21</sup> The values for  $Q_{\text{Cu}}$  and  $Q_{\text{Co}}$  were determined using current transient curves as exemplified in Fig. 1(b). According to our chronoamperometry analysis, the current efficiency for Co is  $\eta_{\text{Co}}\sim 80\%$ , although the value for Cu can be assumed to be  $\eta_{\text{Cu}}\sim 100\%$ .<sup>21,22</sup> The deposition rates for different wires in a sample may not be entirely uniform, which was indeed found in Co/Cu nanowire samples according to our microstructural analysis using scanning electron microscopy (SEM), as de-

TABLE I. A summary of electrodeposition conditions of Co/Cu nanowires along with the measured values of GMR and magnetic fields  $H_p$  which give the maximum MR value. Samples 1 and 2 have the same Co and Cu layer thicknesses grown at the different Cu deposition potentials. Samples 3 and 4 have the same Cu layer thickness with different Co layer thicknesses. The bold numbers highlight the differences.

Sample ID	1	2	3	4
V (Co) (V)	-1.0	-1.0	-1.0	-1.0
Co layer thickness (nm)	11±1	11±1	<b>8±1</b>	<b>3±0.5</b>
V (Cu) (V)	<b>-0.5</b>	<b>-0.3</b>	-0.3	-0.3
Cu layer thickness (nm)	6±0.5	6±0.5	10±1	10±1
CPP-GMR	9.6±0.2%	7.3±0.2%	13.5±0.2%	8.3±0.2%
$H_p$ (Oe) (perpendicular)	200±4	320±5	196±5	95±3
$H_c$ (Oe) (perpendicular)	...	...	195±2	20±2

scribed later. We also found that the total deposition charge monitored when the first wire grew to the end of a pore was smaller than the expected charge that was needed to fill up all the pores of the template. Thus, the estimated layer thickness by the method shown above was close to the actual layer thickness of the longest wires that have grown to the end of the pores and were characterized through CPP-GMR, but was larger than the average layer thickness of all the wires (including those that have not grown to the end of the pores) in the template.

In order to explain the effects of interface and Co layer thickness on the CPP-GMR in Co/Cu nanowires, four representative samples numbered from 1 to 4, prepared in different growth conditions, are selected from a number of samples that we prepared and characterized. Samples 1 and 2 are Co/Cu nanowires of the same Co and Cu layer thicknesses grown at the same deposition potential for Co but at different potentials for Cu. Samples 1 and 2 are used to discuss the effects of interface roughness and/or intermixing on the CPP-GMR effect. Samples 3 and 4 have the same layer thickness for Cu but different values for Co grown at the same deposition potentials for Co and Cu. Samples 3 and 4 are used to discuss the effects of the magnetic Co layer thickness on the CPP-GMR. The deposition potentials, layer thicknesses, room-temperature CPP-GMR, and the magnetic fields  $H_p$  which give the maximum MR values for all these samples are summarized in Table I.

## B. SEM and XRD of nanowires

The structure of the electrodeposited Co/Cu-multilayered nanowires was examined using SEM. Prior to SEM observation of Co/Cu nanowires, the alumina templates used for the nanowire growth were mechanically forced to break. The image in Fig. 2(a) clearly shows the well-aligned nanowires with  $\sim 300$  nm diameter, which confirms that the nanowires were indeed electrodeposited inside the pores of the template. However, the lengths of as-grown nanowires are not uniform, indicating that only the longest nanowires, which have contacted the Au film coated on the other ends of the pores, contribute to the MR change. It should be noted that the sample shown in Fig. 2 was deliberately grown in short lengths for ease of SEM observation ( $< 10 \mu\text{m}$ ). The narrower pores as indicated by the arrows in Fig. 2(a) are the part of the template that ends with the

100 nm branches of pores. The surface along the direction of the nanowire axis is smooth in the image with 50 000 magnification [see Fig. 2(b)] and many terminating surfaces of nanowires are perpendicular to the long axis of nanowire. This implies that the interfaces of Cu and Co most likely are perpendicular to the growth direction of the nanowire. According to the peak intensity positions in x-ray-diffraction (XRD)  $\theta$ - $2\theta$  data (not shown here), our Co/Cu nanowires have the face-centered-cubic (fcc) structure with a strong (111) texture along the growth direction of nanowires. No superlattice satellite peaks were observed from the  $\theta$ - $2\theta$  scan, probably because of a variation of bilayer thickness in the nanowires.

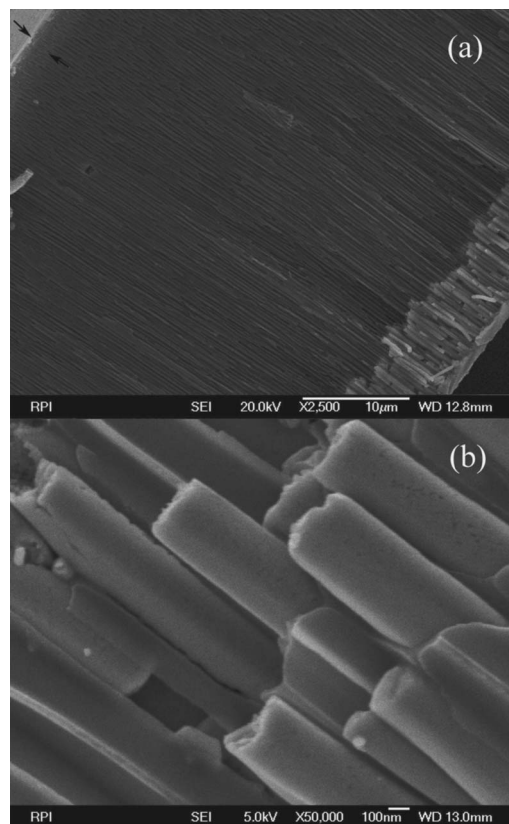


FIG. 2. SEM images of electrodeposited Co(-1.0 V, 15 nm)/Cu(-0.5 V, 15 nm)-multilayered nanowires taken at (a) low magnification ( $\times 1500$ ) and (b) high magnification ( $\times 50\,000$ ). The growth of wires was deliberately stopped short for easy observation of length variation in wires.

### C. Magnetotransport measurements

The MR of Co/Cu nanowires was measured using a PC-controlled magnetotransport measurement system. The MR measurements of the nanowires were carried out at room temperature using a two-point contact method in the magnetic fields up to 9 kOe. To make the two-point contact for the MR measurements, the Au-coated side (100 nm pore size) of the nanowires was connected with a Cu wire using a silver epoxy and the Cu-coated side (300 nm pore size) with a conducting tape. The approximate number of nanowires electrically contacted can be estimated from the measured resistance of Co/Cu nanowire samples. We estimated that the resistance of a single nanowire in Co/Cu nanowires is in the order of a few tens to a few hundreds ohms, depending on the values of resistances for individual Co and Cu layers and the interfacial resistance between the Co and Cu layers presented in the reference.<sup>21</sup> In the case of the Co/Cu nanowire samples we studied, the net resistance of the nanowires was in the range of 20–130  $\Omega$ , indicating that only a few nanowires were actually contacted and contributed to the magnetoresistance in the parallel resistance configuration. This estimate is consistent with the SEM result shown in Fig. 2 that some nanowires will not grow to the end of the pores if the electrodeposition continues.

Figure 3 shows the MR curves for samples 1 and 2 measured in a magnetic field applied either perpendicular or parallel to the wire axes. It should be noted again that the Cu deposition potentials used for the growth of these samples were different (–0.5 and –0.3 V for samples 1 and 2, respectively), while the Co deposition potentials were the same. The change in the Cu deposition potential apparently results in different shapes of the MR curve. The MR curves for sample 2 grown at –0.3 V for Cu exhibit a maximum at  $H_p=320$  Oe which is larger than  $H_p=200$  Oe for that of sample 1 grown at –0.5 V for Cu, even though the MR changes of sample 1 (9.6%) and sample 2 (7.3%) are not very different. Figure 4 shows the MR curves and the magnetization hysteresis loops (see inset) for sample 3 and sample 4 measured in magnetic fields perpendicular or parallel to the wire axes. These samples were deposited at the same Cu (–1.0 V) and Co (–0.3 V) potentials with different Co layer thicknesses. Sample 3, having Cu and Co layer thicknesses of 10 nm and 8 nm, respectively, shows a MR change of 13.5%, which is the highest value we have measured so far. A much smaller  $H_p$  value was observed for sample 4 having the Co layer thickness of 3 nm, which is smaller than that of sample 3. It can be seen from Figs. 3 and 4 that CPP-GMR value slightly changed when a magnetic field was applied parallel to the nanowire axes. This is because the anisotropic magnetoresistance (AMR) was superposed on the measured CPP-GMR value.

### III. DATA ANALYSIS AND DISCUSSIONS

#### A. Effects of interfacial mixing and roughness on GMR

The observed difference in the shape of the MR curves for samples 1 and 2 may be attributed to the difference in the interfacial structure of these two Co/Cu nanowire samples. It

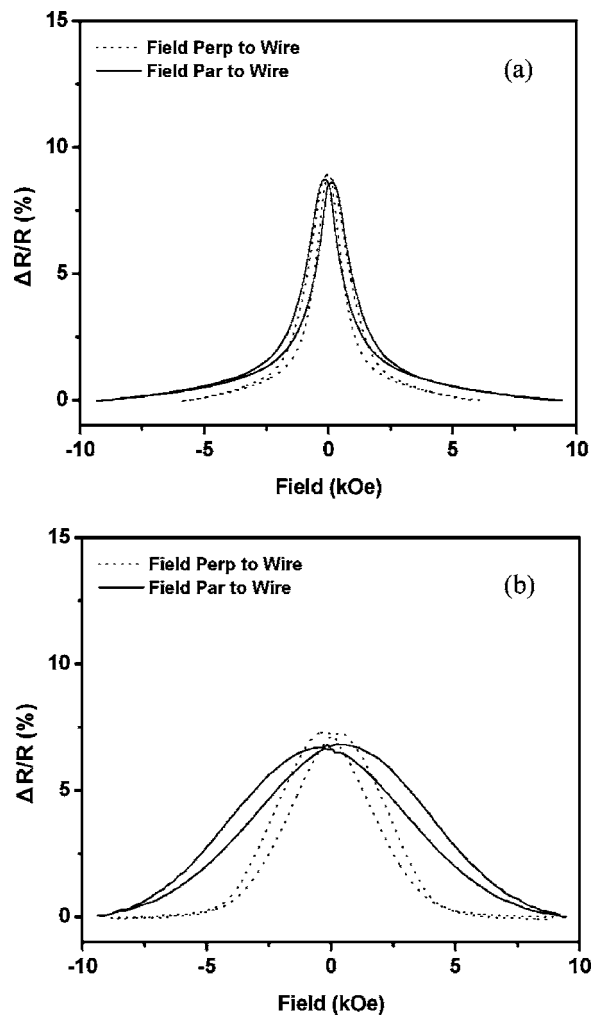


FIG. 3. Magnetoresistance curves for Co/Cu nanowires of (a) sample 1 and (b) sample 2 measured in magnetic fields applied perpendicular (dashed curve) and parallel (solid curve) to the wire axes. These two samples have the same Co and Cu layer thickness grown at the same deposition potential for Co but at different potentials for Cu. The Cu deposition potentials for sample 1 and sample 2 are –0.5 and –0.3 V, respectively.

has been found that there is an exchange reaction between the noble metal (Cu) and magnetic metal (Ni or Co) during the pulsed electrodeposition of Ni/Cu or Co/Cu-multilayered thin films using a single bath.<sup>13–16</sup> The exchange reaction also happens in the electrodeposition of multilayered nanowires. This effect will result in a chemically intermixed interface between the noble and magnetic metals.<sup>12</sup> The intermixing at the Co/Cu interfaces is also probably energetically favorable because such an alloying can decrease the interfacial free energy.<sup>23,24</sup> The exchange reaction is more significant for the Co/Cu system than the Ni/Cu system,<sup>6</sup> because the difference in standard electrode potentials, which is the driving force of this reaction, is higher in the case of the Co/Cu system.<sup>13</sup> The exchange reaction between Co and  $\text{Cu}^{2+}$  ( $\text{Co} + \text{Cu}^{2+} \rightarrow \text{Co}^{2+} + \text{Cu}$ ) takes place because the reduction potential of  $\text{Cu}^{2+}$  is more positive than the oxidation potential of Co.<sup>25</sup> The strength of the exchange reaction changed with the Cu deposition potential, where anodic dissolution of Co significantly increases with increasing the potential to the positive values. At

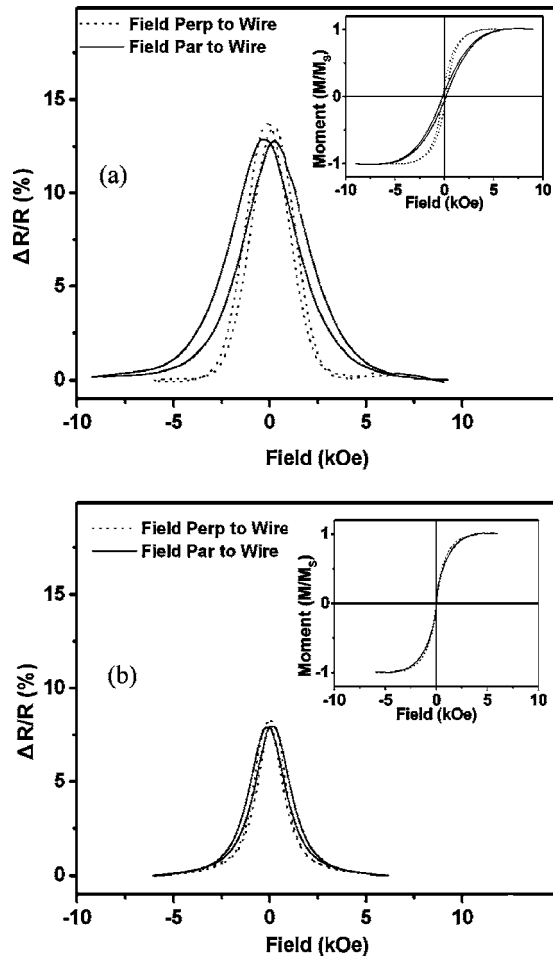


FIG. 4. Magnetoresistance curves for Co/Cu nanowires of (a) sample 3 and (b) sample 4 measured in magnetic fields applied perpendicular (dashed curve) and parallel (solid curve) to the wire axes. The inset shows the magnetization hysteresis loops. These two samples have the same Cu layer thickness but different Co layer thicknesses. Samples were grown at the same deposition potentials for Co and Cu. The Co layer thickness for sample 3 and sample 4 are 8 and 3 nm, respectively.

$U = -0.5$  V for the Cu deposition, anodic dissolution of Co is negligibly small, while at  $U = -0.3$  V the Co dissolution is significant, as indicated in Fig. 1(b). Correspondingly, the interfacial structure of electrodeposited Co/Cu multilayers changed by varying the Cu deposition potential. Sample 2, which has Cu layers deposited at  $U = -0.3$  V, may have rougher interfaces or more intermixing at the interfaces than sample 1 with Cu layers grown at  $U = -0.5$  V.

Although sample 2 is expected to have rougher and more intermixed interfaces than sample 1, their MR changes are not much different (9.6% for sample 1 and 7.3% for sample 2). This observation cannot be explained by a mechanism previously reported for multilayered Co/Cu thin films where an interfacial intermixing was found to significantly decrease the GMR effect.<sup>20</sup> The decrease in the GMR effect for Co/Cu thin films with increasing interfacial roughness is due to the reduced antiferromagnetic coupling between Co layers. On the other hand, both samples 1 and 2 we studied have the Cu layer thickness of  $\sim 6$  nm which does not give rise to any significant antiferromagnetic coupling between the layers. The magnetic layers are in the uncoupled region when

the Cu layer thickness is larger than 3 nm.<sup>26</sup> In this case, the magnetizations in the Co layers are randomly aligned, instead of an antiferromagnetically (AF) or ferromagnetically ( $F$ ) aligned as expected from the Ruderman-Kittel-Kasuya-Yoshida (RKKY) interaction.<sup>27-29</sup> Because the magnetic layers of Co/Cu nanowires are not exchange coupled between them, interfacial mixing will not significantly affect the coupling to reduce the GMR effect. We speculate that the physical origin of the CPP-GMR for the uncoupled Co/Cu nanowire system is somewhat similar to that of antiferromagnetically coupled Co/Cu thin films.<sup>30</sup> In zero magnetic field, the magnetization in randomly oriented domains in the magnetic layers may have an effect very similar to that of the antiparallel alignment; both the spin-up and spin-down electrons are strongly scattered in the Co layers that have a magnetization direction opposite to their spin direction to give a larger resistance. When the magnetic field is increased, the magnetic moments begin to be aligned to the field direction and hence to decrease the resistance.

Since sample 2 is expected to have rougher interfaces than sample 1, there should be more scattering centers at the interface. If the scattering at the interface is strongly spin dependent, sample 2 should have a larger GMR value. However, the GMR effect observed in sample 2 was in fact smaller than in sample 1, indicating that the scattering occurring at the interfaces is not strongly spin dependent. The interfacial scattering may rather contribute to the residual resistance of the sample and only slightly decreases the GMR ratio.

The effects of interfacial roughness and intermixing on the increased saturation field in our Co/Cu nanowires also cannot be explained by the mechanism used for Co/Cu multilayer thin films<sup>20</sup> because the magnetic layers of the nanowires are not exchange coupled. For an antiferromagnetically coupled Co/Cu system, the saturation field may decrease with increasing interfacial mixing because the mixing reduces the antiferromagnetic interlayer coupling. However, the interface mixing will not influence the coupling between the uncoupled Co layers since they are randomly aligned anyway. The increase in the  $H_p$  value and the saturation field with increasing interfacial mixing could be due to the increased number of pinning sites at the interface.<sup>24,31</sup> Roughness of interfaces in the multilayer may result in reducing the uniformity of the layer thicknesses and introducing defects such as dislocations and step edges at the interface.

## B. Optimum thickness for high GMR

A MR change of 13.5% was observed from sample 3, which contains Co(8 nm)/Cu(10 nm) nanowires, which is the highest value observed among the samples we measured, indicating that Co(8 nm)/Cu(10 nm) is the optimum layer thicknesses to achieve a highest GMR ratio in  $\sim 300$  nm diameter nanowires. The CPP-GMR effect is generally larger than the CIP-GMR effect in this relatively large layer thickness range because the scaling length for the CIP-GMR is different from that for the CPP-GMR. Namely, for the CIP-GMR, the scaling length is the electron mean free path, while for the CPP-GMR, according to Valet-Fert (VF)

model,<sup>32,33</sup> the scaling length is the spin-diffusion length due to the spin accumulation effect which is related to the spin-flip mean free path. The spin-diffusion length can be much larger than the electron mean free path, thus the CPP-GMR effect can be observed for multilayers with larger layer thicknesses. When the layer thicknesses are smaller than 10 nm for Cu layers or 8 nm for Co layers, anodic dissolution of Co more significantly influences the interfacial roughness and intermixing, leading to a decreased GMR effect. When the Co layer thicknesses further increases, the GMR effect decreases, which agrees with the VF model. When the Cu layer thickness is increased to values larger than 10 nm, the resistance in the nonmagnetic layers increases, which is an effect similar to an increase in the contact resistance and a decrease in the MR change. The MR change of 13.5% obtained for Co(8 nm)/Cu(10 nm) nanowires in our alumina templates is close to the values of 11% observed by Liu *et al.*<sup>9</sup> and of 15% reported by Piraux *et al.*<sup>10</sup> on electrodeposited Co/Cu nanowires made using polycarbonate templates with diameters of 40 and 30 nm, respectively.

### C. $H_p$ from peak MR

A much smaller  $H_p$  value (95 Oe) was obtained for sample 4 than that for sample 3 (196 Oe); a similar trend was observed in the coercivity  $H_c$  of the magnetic hysteresis curves measured for the same samples, where the coercivities for samples 4 and 3 are 20 and 195 Oe, respectively (see Table I). It is interesting to note that Cerisier *et al.* have reported a different trend in Co thin films grown on a (111)-textured Cu surface from what we observed in Co/Cu nanowires.<sup>34</sup> They found that coercivity increases with decreasing film thickness where a linear increase of  $H_c$  from 25 to 192 Oe was observed when the Co layer thickness decreased from 200 to 2.5 nm. The smaller values of  $H_p$  and  $H_c$  we obtained for sample 4 with the smaller layer thickness may be related to the anodic dissolution of Co and to the intermixing at the interfaces. These interfacial effects may not be negligible when the Co layer thicknesses are very small as they result in a nonuniform Co layer thickness. In very thin layer thickness of Co, the Co may become discontinuous in the Cu matrix, which may give a coercivity close to that of the bulk Co.<sup>16</sup> The minimum thickness of continuous Co layers reliably produced in multilayers may be 3 nm.<sup>26</sup> This limitation in fabricating continuous layers of Co/Cu nanowires may be related to anodic dissolution of Co during electrodeposition.

It should be pointed out that the  $H_p$  value observed at a maximum MR and the  $H_c$  value obtained from the magnetic hysteresis loop could be very different. For example, the  $H_p$  and  $H_c$  values for sample 4 are 95 and 20 Oe, respectively. Such a difference could be observed because basically the GMR effect is measured only for the nanowires grown to the end of the pores and electrically contacted for measurements, while magnetic hysteresis curves are measured for all the nanowires grown. Hence, the layer thicknesses of the nanowires that served for the CPP-GMR measurements are probably larger than the average layer thicknesses of all the wires that served for the magnetic hysteresis curves.

### D. Easy axis in the direction perpendicular to the nanowire axis

All the CPP-GMR data we obtained indicate that the magnetic easy axes of the nanowires are in the plane perpendicular to the wire axes as the MR value reaches saturation in a magnetic field smaller in the direction perpendicular to the wire axes than that in the direction parallel to them. This trend is also confirmed by the magnetic hysteresis curve measurements; the magnetic easy axes were in the plane perpendicular to the wire axes. For sample 4, the anisotropy indicated by both GMR curve and magnetic hysteresis curve is weak. This is possibly due to the discontinuity in its Co layer as discussed in Sec. III C.

The magnetic easy axes reflect various magnetic anisotropies including the magnetocrystalline and shape anisotropies. In the case of thin films, the easy axis often lies in the plane of the film due to the shape anisotropy. The disk-shaped magnetic layers in a multilayered nanowire can be considered as an oblate spheroid with a small aspect ratio  $R$  defined as the ratio of the layer thickness to the diameter.<sup>35</sup> The demagnetizing factor for such a thin layer is nearly unity in the direction parallel to the wire axis and zero in directions perpendicular to the wire axis, and the shape anisotropy constant is  $\sim 2\pi M_s^2$ .<sup>35</sup> The saturation magnetization  $M_s$  for Co layers may be very close to that for the bulk (1424 emu/cm<sup>3</sup>).<sup>36</sup> In the Co–Cu series, the average saturation magnetization is 1241 emu/cm<sup>3</sup> as  $M_s$ ,<sup>37</sup> thus, the shape anisotropy energy  $2\pi M_s^2$  is about  $9.7 \times 10^6$  erg/cm<sup>3</sup>. The magnetocrystalline anisotropy for a cubic system can be represented by the first two terms with anisotropy constants  $K_1$  and  $K_2$ . To estimate the magnetocrystalline anisotropy for Co layers in Co/Cu nanowires, the values obtained for Co–Pd alloyed films<sup>38</sup> were used; in the Co-rich-alloyed films the values for  $E_a\langle 111 \rangle - E_a\langle 100 \rangle$  and  $E_a\langle 110 \rangle - E_a\langle 100 \rangle$  are about  $-4 \times 10^5$  and  $-3 \times 10^5$  erg/cm<sup>3</sup> respectively. The estimated anisotropy constants  $K_1$  and  $K_2$  are around  $-1.2 \times 10^6$  and 0 erg/cm<sup>3</sup>, respectively. If only the magnetocrystalline anisotropy should be considered, the easy axis should then lie along the  $\langle 111 \rangle$  directions. The actual magnetocrystalline anisotropy constants for Co/Cu nanowire systems may be different;  $K_1$  is<sup>39</sup>  $-0.85 \times 10^6$  or<sup>40</sup>  $-1.2 \times 10^6$  erg/cm<sup>3</sup>. In these multilayer systems, the magnetocrystalline anisotropy is generally much smaller than the shape anisotropy that is responsible for orienting the easy axis to the direction parallel to the film plane (perpendicular to the wire axes).

### IV. CONCLUSIONS

We have demonstrated that multilayered Co/Cu nanowires grown by a pulsed electrodeposition using porous alumina templates are an ideal system to investigate the CPP-GMR. When the potential is switched for Cu deposition, anodic dissolution of Co and an intermixing may occur, leading to interfacial roughness and/or intermixing at Co/Cu interfaces, sensitively depending on the potential chosen for Cu. SEM study of the samples showed the structure of the high aspect ratio nanowires and the nonuniform wire lengths. The Co/Cu nanowires are in a fcc structure with the (111) texture. The anodic dissolution of Co and intermixing at the

interfaces does not significantly decrease the CPP-GMR ratio of the Co/Cu nanowires that have randomly coupled Co layers. The Cu layer thickness of about 10 nm and Co layer thickness of about 8 nm are optimum values to show a large GMR effect. The Co/Cu nanowires have an easy axis in the plane perpendicular to the wire axes due to the predominant shape anisotropy in the disk-shaped magnetic layers in the nanowires.

## ACKNOWLEDGMENTS

The work was supported by a RPI Seed Grant. We thank F. Tang for discussions and reading of the manuscript.

- <sup>1</sup>D. A. Thompson and J. S. Best, *IBM J. Res. Dev.* **44**, 311 (2000).
- <sup>2</sup>A. Barthélémy *et al.*, *J. Magn. Magn. Mater.* **68**, 242 (2002).
- <sup>3</sup>H. Schwanbeck and U. Schmidt, *Electrochim. Acta* **45**, 4389 (2000).
- <sup>4</sup>P. Aranda and J. M. García, *J. Magn. Magn. Mater.* **249**, 214 (2002).
- <sup>5</sup>H. Masuda and K. Fukuda, *Science* **268**, 1466 (1995).
- <sup>6</sup>C. A. Ross, *Annu. Rev. Mater. Sci.* **24**, 159 (1994).
- <sup>7</sup>M. Shima, L. Salamanca-Riba, T. P. Moffat, R. D. McMichael, and L. J. Swartzendruber, *J. Appl. Phys.* **84**, 1504 (1998).
- <sup>8</sup>M. Shima, L. Salamanca-Riba, T. P. Moffat, and R. D. McMichael, *J. Magn. Magn. Mater.* **199**, 52 (1999).
- <sup>9</sup>K. Liu, K. Nagodawithana, P. C. Searson, and C. L. Chien, *Phys. Rev. B* **51**, 7381 (1995).
- <sup>10</sup>L. Piraux, J. M. George, J. F. Despres, C. Leroy, E. Ferain, R. Legras, K. Ounadjela, and A. Fert, *Appl. Phys. Lett.* **65**, 2484 (1994).
- <sup>11</sup>W. Schwarzacher, K. Attenborough, A. Michel, G. Nabiyouni, and J. P. Meier, *J. Magn. Magn. Mater.* **165**, 23 (1997).
- <sup>12</sup>M. Shima, L. Salamanca-Riba, and T. P. Moffat, *Electrochem. Solid-State Lett.* **2**, 271 (1999).
- <sup>13</sup>L. Peter *et al.*, *J. Electrochem. Soc.* **148**, C168 (2001).
- <sup>14</sup>I. Bakonyi, J. Tóth, L. Goualou, T. Becsei, E. Tóth-Kádár, W. Schwarzacher, and G. Nabiyouni, *J. Electrochem. Soc.* **149**, C195 (2002).
- <sup>15</sup>G. Nabiyouni, W. Schwarzacher, Z. Rolik, and I. Bakonyi, *J. Magn. Magn. Mater.* **253**, 77 (2002).
- <sup>16</sup>Q. X. Liu, L. Péter, J. Tóth, L. F. Kiss, Á. Cziráki, and I. Bakonyi, *J. Magn. Magn. Mater.* **280**, 60 (2004).
- <sup>17</sup>E. E. Fullerton, D. M. Kelly, J. Guimpel, I. K. Schuller, and Y. Bruynseraede, *Phys. Rev. Lett.* **68**, 859 (1992).
- <sup>18</sup>R. Schad, P. Beliën, G. Verbanck, V. V. Moshchalkov, Y. Bruynseraede, H. E. Fischer, S. Lefebvre, and B. Bessiere, *Phys. Rev. B* **59**, 1242 (1999).
- <sup>19</sup>H. Kano, K. Kagawa, A. Suzuki, A. Okabe, K. Hayashi, and K. Asoa, *Appl. Phys. Lett.* **63**, 2839 (1993).
- <sup>20</sup>M. Suzuki and Y. Taga, *J. Appl. Phys.* **74**, 4660 (1993).
- <sup>21</sup>A. Fert and L. Piraux, *J. Magn. Magn. Mater.* **200**, 338 (1999).
- <sup>22</sup>W. Schwarzacher and D. S. Lashmore, *IEEE Trans. Magn.* **32**, 3133 (1996).
- <sup>23</sup>J. Camarero *et al.*, *Surf. Sci.* **402**, 346 (1998).
- <sup>24</sup>Q. Jiang and G.-C. Wang, *J. Vac. Sci. Technol. B* **14**, 3180 (1996).
- <sup>25</sup>P. Fricoteaux and J. Douglade, *Surf. Coat. Technol.* **184**, 63 (2004).
- <sup>26</sup>B. Voegeli, A. Blondel, B. Doudin, and J.-Ph. Ansermet, *J. Magn. Magn. Mater.* **151**, 388 (1995).
- <sup>27</sup>M. A. Ruderman and C. Kittel, *Phys. Rev.* **96**, 99 (1954).
- <sup>28</sup>T. Kasuya, *Prog. Theor. Phys.* **16**, 4558 (1956).
- <sup>29</sup>I. Yosida, *Phys. Rev.* **106**, 893 (1957).
- <sup>30</sup>E. Y. Tsymlal and D. G. Pettifor, in *Solid State Physics*, edited by H. Ehrenreich and F. Spaepen (Academic, San Diego, 2001), Vol. 56, pp. 113–237.
- <sup>31</sup>Q. Jiang, H.-N. Yang, and G.-C. Wang, *Surf. Sci.* **373**, 181 (1997).
- <sup>32</sup>T. Valet and A. Fert, *Phys. Rev. B* **48**, 7099 (1993).
- <sup>33</sup>A. Fert, T. Valet, and J. Barnas, *J. Appl. Phys.* **75**, 6693 (1994).
- <sup>34</sup>M. Cerisier, K. Attenborough, J.-P. Celis, and C. Van Haesendonck, *Appl. Surf. Sci.* **166**, 154 (2000).
- <sup>35</sup>L. Sun, Y. Hao, C.-L. Chien, and P. C. Searson, *IBM J. Res. Dev.* **49**, 79 (2005).
- <sup>36</sup>W. Weber, A. Bischof, and R. Allenspach, *Phys. Rev. B* **54**, 4075 (1996).
- <sup>37</sup>C. H. Lee, H. He, F. J. Lamelas, W. Vavra, C. Uher, and Roy Clarke, *Phys. Rev. B* **42**, 1066 (1990).
- <sup>38</sup>H. Fujiwara, H. Kadomatsu, and T. Tokunaga, *J. Magn. Magn. Mater.* **809**, 31 (1983).
- <sup>39</sup>J. Fassbender, Ch. Mathieu, B. Hillebrands, G. Giintherodt, R. Jungblut, and M. T. Johnson, *J. Appl. Phys.* **76**, 6100 (1994).
- <sup>40</sup>D. S. Chuang, C. A. Ballentine, and R. C. O'Handley, *Phys. Rev. B* **49**, 15084 (1994).